RESEARCH ARTICLE

Journal of Cellular Physiology WILEY

Thrombospondin-1 mediates Rho-kinase inhibitor-induced increase in outflow-facility

Sze-Wan Shan[1] | Chi-Wai Do[1,2] | Thomas Chuen Lam[1,2,3] | Hoi-Lam Li[1] | W. Daniel Stamer[4,5] | Chi-Ho To[1,2]

[1]Laboratory of Experimental Optometry, School of Optometry, The Hong Kong Polytechnic University, Hong Kong, China

[2]Centre for Eye and Vision Research, Hong Kong, China

[3]The Hong Kong Polytechnic University Shenzhen Research Institute, Shenzhen, Guangdong, China

[4]Department of Ophthalmology, Duke University, Durham, North Carolina, USA

[5]Department of Biomedical Engineering, Duke University, Durham, North Carolina, USA

Correspondence
Dr. Chi-Wai Do and Dr. Thomas Chuen Lam, Laboratory of Experimental Optometry, School of Optometry, The Hong Kong Polytechnic University, Hong Kong, China.
Email: chi-wai.do@polyu.edu.hk and thomas.c.lam@polyu.edu.hk

Funding information
The Hong Kong Polytechnic University Internal Grants, Grant/Award Numbers: SB78, UAGF, UAHG; RGC General Research Fund, Grant/Award Numbers: 15104819, PolyU151020/15M; Shenzhen Science and Technology Innovation Commission, Grant/Award Number: JCYJ20180507183409601; PolyU Postgraduate Studentship, Grant/Award Number: H.L.L; The Hong Kong Polytechnic University, Grant/Award Number: Henry G Leong Professorship in Elderly Vision Health

Abstract

Rho-kinase (ROCK) inhibitors, a novel class of anti-glaucoma agents, act by increasing the aqueous humor outflow through the conventional trabecular meshwork pathway. However, the downstream signaling consequences of the ROCK inhibitor are not completely understood. Our data show that Y39983, a selective ROCK inhibitor, could induce filamentous actin remodeling, reduced cell motility (as measured by cell migration), and transepithelial resistance in primary human TM (hTM) cells. After 2 days Y39983 treatment of hTM cells, a proteomic study identified 20 proteins whose expression was significantly altered. Pathway analysis of those proteins revealed the involvement of the p53 pathway, integrin signaling pathway, and cytoskeletal pathway regulation by Rho GTPase. Thrombospondin-1 (TSP1), a matricellular protein that is increased in glaucoma patients, was downregulated fivefold following Y39983 treatment. More importantly, both TSP1 antagonist leucine–serine–lysine–leucine (LSKL) and small interfering RNA (siRNA) reduced TSP1 gene and protein expressions as well as hTM cell migration. In the presence of Y39983, no further inhibition of cell migration resulted after LSKL and TSP1 siRNA knockdown. Likewise, LSKL triggered a dose-dependent increase in outflow facility in ex vivo mouse eyes, to a similar extent as Y39983 (83.8% increase by Y39983 vs. 71.2% increase by LSKL at 50 μM). There were no additive effects with simultaneous treatment with LSKL and Y39983, supporting the notion that the effects of ROCK inhibition were mediated by TSP1.

KEYWORDS
glaucoma, outflow facility, ROCK inhibitor, thrombospondin-1, trabecular meshwork

1 | INTRODUCTION

The trabecular meshwork (TM) is a specialized ocular tissue located in the anterior chamber angle. It is responsible for the conventional outflow facility, accounting for more than 80% of the aqueous humor drainage in human eyes (Bill & Phillips, 1971; Jocson & Sears, 1971), and thereby playing an important role in the regulation of intraocular pressure (IOP). Glaucoma is typically characterized by IOP elevation due to an increased outflow resistance (Fatma et al., 2009; Lingor et al., 2008). The regulation of the outflow facility is complicated and

may involve multiple interdependent mechanisms. Outflow resistance can be affected by several factors, including ciliary muscle tone, TM cell contractility, and extracellular matrix (ECM) status. ECM proteins including collagen, laminin, fibronectin, glycosaminoglycans (GAGs), and matricellular proteins are found in the TM. The composition of ECM and its equilibrium is a major determinant of the outflow resistance, and abnormal ECM deposition is a common feature of glaucomatous eyes (Alvarado et al., 1986; Rohen, 1983).

Rho guanosine triphosphatase (GTPase) plays an important role in regulating various cellular functions, including cell morphology, cytoskeletal rearrangement, smooth muscle contraction, and cell motility (Kaibuchi et al., 1999; Nobes & Hall, 1995). These functions are mediated by its downstream Rho effectors, such as Rho-associated protein kinase (ROCK; Fukata et al., 2001; Honjo et al., 2001). ROCK-mediated changes in TM cell contractility (Rao et al., 2005), focal adhesions (Rao et al., 2001), disruption of actin fibers (Dang et al., 2019), and alterations of associated giant vacuoles and tight junctions in Schlemm's canal (SC) cells (Kameda et al., 2012) are associated with increased conventional outflow facility and IOP lowering (Kaneko et al., 2016; Rao et al., 2001). Y27632 is the first ROCK inhibitor shown to lower IOP in rabbit eyes (Honjo et al., 2001), suggesting that inhibition of the ROCK pathway may be a viable therapeutic strategy for glaucoma. Subsequently, it has been demonstrated that Y39983, an analog of Y27632, has an IC$_{50}$ ~30 times lower than that of Y27632 in inhibiting ROCK activity (Tokushige et al., 2007). The IOP-lowering effect exerted by Y39983 is found to be ~10 times higher than that by Y27632 (Tokushige et al., 2007). Recently, ripasudil hydrochloride hydrate (K-115) became the first ROCK inhibitor developed for the treatment of glaucoma and ocular hypertension in Japan (Garnock-Jones, 2014), while netarsudil (AR-13324) has been approved by the Food and Drug Administration in the United States for lowering IOP clinically (Mehran et al., 2020). Despite these advances, the precise cellular downstream events mediated by ROCK inhibitors in TM cells are not yet fully understood.

Transforming growth factor-β (TGF-β) has long been implicated in glaucoma pathogenesis because patients with primary open-angle glaucoma (POAG) and angle-closure glaucoma demonstrate an elevated level of TGF-β in the aqueous humor (Chen et al., 2020; Fuchshofer & Tamm, 2012; Inatani et al., 2001). TGF-β alters the expression and deposition of ECM in the TM, leading to an increased outflow resistance due to excessive accumulation and fibrotic changes of ECM in TM cells (Wallace et al., 2014). Thrombospondin-1 (TSP1) is a matricellular protein that has been associated with glaucoma pathophysiology through TGF-β pathway activation (Flugel-Koch et al., 2004; Kuchtey et al., 2014). TSP1 is involved in regulating cell adhesion, cytoskeleton, and ECM homeostasis. It has been demonstrated that leucine–serine–lysine–leucine (LSKL) peptide, a TSP1 antagonist, is a latency-associated protein (LAP)-TGF-β derived peptide. LSKL competitively blocks TGF-β activation by inhibiting the binding of TSP1 to LAP, causing a reduction of the active form of TGF-β (Belmadani et al., 2007). The primary goal of this study was to evaluate the role of TSP1 in triggering the Y39983-mediated responses in TM cells and outflow facility.

2 | MATERIALS AND METHODS

2.1 | Human TM cell culture

Human TM (hTM) cells, which had been characterized previously, were obtained from the Duke University School of Medicine (Snyder et al., 1993; Stamer et al., 1995). Human tissues were processed in accordance with the tenets of the Declaration of Helsinki. Cell strains from five donors of both sexes (3-month-old/female/donor whole globe, 11-month-old/unknown sex/donor whole globe, 39-year-old/male/corneal rim, 75-year-old/female/donor whole globe, 88-year-old/female/corneal rim; at the third or fourth subculture) were used according to the consensus recommendations (Keller et al., 2018). Cells were plated and incubated at 37°C until confluence and subsequently maintained in Dulbecco's modified Eagle's medium (DMEM, low glucose; Invitrogen), containing penicillin (100 units/ml), streptomycin (100 mg/ml), glutamine (0.29 mg/ml), and 1% fetal bovine serum (FBS; Invitrogen) for at least a week before the experiments.

2.2 | Immunohistochemistry of actin cytoskeleton

hTM cells were incubated with a serum-free medium overnight. Subsequently, 1 μM Y39983 (MedChem Express) was added and incubated for 2 days at 37°C. The hTM cells were then fixed with 2% paraformaldehyde for 30 min, washed with phosphate-buffered saline (PBS), and incubated with fluorescein-phalloidin (Invitrogen-Molecular Probes) for 30 min. The stained cells were then washed and observed under a fluorescence microscope.

2.3 | Measurement of cell motility

Confluent monolayers of hTM cells were subjected to a migration assay as described previously (Shan et al., 2009). Cells were scraped to create a linear gap, followed by replacing the medium with 0.25% FBS–DMEM, with or without Y-39983 or with LSKL peptide, a selective TSP1 blocking peptide or serine–leucine–leucine–lysine (SLLK) peptide, an inert control. Both control and blocking peptides were purchased from AnaSpec. The movement of hTM cells into the gap area was photographed at designated time points. The gap area was calculated using ImageJ (version 1.49) software and represented as a percentage of the initial gap area.

In addition, cell motility was monitored by a transwell migration assay. Cells transfected with small interfering RNAs (siRNAs), blocking peptide or control peptide-treated hTM cells (5 × 10^4 cells per well) were seeded in the upper chamber of the transwell plates in FBS-free media with membrane inserts. Six hundred microlitres of DMEM supplemented with Y39983 (1 μM) was added to the lower compartments of the plate. The plate was incubated at 37°C for 48 h.

Migrated cells were fixed, and stained with 0.05% crystal violet. The inserts were washed with PBS and dried before capturing images.

2.4 | Transepithelial electrical measurements

hTM cells were cultured on Snapwell inserts (Costar; Corning Incorporated) at a density of 4×10^5 cells/ml. The preparation was mounted in an Ussing Chamber System (Physiologic Instruments) containing Ringer's solution on both sides at room temperature (Cheng et al., 2016). After that, bilateral application of Y39983 at various concentrations (1, 10, and 50 μM) were added to the bathing solution sequentially and treated for 1 h at each concentration. Subsequent to blank resistance subtraction, changes in transepithelial electrical resistance (TER) were continuously monitored by a DVC-1000 (World Precision Instruments) to evaluate the changes in permeability of hTM cell layers.

2.5 | Liquid chromatography–mass spectrometry (MS)/MS

2.5.1 | Bioinformatics data analysis

The detailed methodology of mass spectrometry (MS) has been described in our technical paper (Shan et al., 2020). Protein identification was performed using the ProteinPilot 5.0 software (SCIEX). The information-dependent acquisition (IDA) data were searched against the human Uniprot database (ver. 26095 entries). Peptide and protein identification were obtained at a 1% false discovery rate (FDR). Only nonredundant proteins were included. The raw MS data (from both data-dependent acquisition and data-independent acquisition) generated in this study were released to the Peptide Atlas public repository (http://www.peptideatlas.org/) for general access (Data ID PASS01254) (Shan et al., 2020). A combined peptide library was constructed by combining all IDAs of each sample. By using SWATH Acquisition MicroApp 2.0 in PeakView 2.0 software (SCIEX), the peptide fragment peaks for each corresponding peptide were extracted. Data were exported to the MarkerView 1.2.1 software (SCIEX) after peak extraction for data normalization and statistical analysis. Differential protein expression was considered significant if the following criteria were fulfilled: fold change of 1.5 and $p \leq 0.05$ (paired Student's *t*-test), protein identification at 1% FDR in ≥2 biological replicates.

2.6 | Reverse transcription-polymerase chain reaction

Similar to our previous study (Li et al., 2018), total RNA was extracted by the Qiagen RNeasy Micro Kit (Qiagen), quantified, and reverse-transcribed to complementary DNA (cDNA) by the High Capacity cDNA Reverse Transcription Kit (Applied Biosystems).

Polymerase chain reaction (PCR) was performed using a HotStarTaq Plus Master Mix Kit (Qiagen) to assess the messenger RNA (mRNA) expression of TSP1. Table S1 shows the primer sequences of target genes used in this study. The primers were designed by the program "Primer3" (http://frodo.wi.mit.edu/primer3/). Following reverse transcription-PCR (RT-PCR) amplification, products were analyzed by agarose gel electrophoresis. The gel image was captured and analyzed by the Azure Imaging System (Azure Biosystems).

2.7 | Downregulation of TSP1 by siRNA

Gene silencing was performed using a TSP1-siRNA and negative control-siRNA. Both TSP1-specific (assay ID s14100) and negative control siRNA were purchased from Invitrogen. This nonsilencing siRNA had no known homology to mammalian genes. The siRNAs were transfected into hTM cells using Lipofectamine 3000 transfection reagent (Invitrogen). After 24-h incubation, the cells were processed for quantitative polymerase chain reaction and cell migration analyses.

2.8 | Real-time quantitative PCR

Reverse transcription of mRNA to cDNA was performed, followed by conducting real-time quantitative PCR (qPCR) using the LightCycler 480 SYBR Green I Master (Roche Applied Science) with primers specific for the target gene *TSP1* (forward primer: 5′-CGTCCTGTTCCTGATGCAT G-3′; reverse primer: 5′-CCAGGAGAGCTTCTTCCACA-3′), and the internal reference gene *GAPDH*. qPCR was performed in 96-well plates on the ROCHE LightCycler 480 (Roche Applied Science). A total reaction volume of 10 μl qPCR mixture containing 5 μl of 2X Taq PCR Master Mix, 1 μl of sterile water, 2 μl of cDNA template, and 1 μl of 10 μM primers (forward and reverse primers, respectively) was used. The thermal cycling conditions were: 95°C for 5 min, followed by 40 cycles of 95°C for 30 s, 61°C for 30 s, and 72°C for 30 s. A melting curve analysis was performed to rule out primer–dimer formation and nonspecific product amplification. For all genes with *GAPDH*, PCR efficiencies (*E*) were determined by analyzing a standard curve ($E = 10^{-1/\text{slope}}$) and compared to ensure similar efficiency ($E = 1.8–2.1$). A negative (i.e., no-template) control sample was included in each plate. Data were analyzed using LightC480 software.

2.9 | Western blot analysis

hTM cells were lysed in lysis buffer containing 7 M urea, 2 M thiourea, 30 mM Tris, 1% ASB14, 2% CHAPS, and protease inhibitor cocktail (Roche). Samples were incubated at 4°C for 1 h with sonication, followed by centrifugation at 13,000*g* for 20 min. After collection of the supernatants, total proteins were quantified by the BioRad Protein Assay (BioRad Laboratories). hTM protein (25 μg) was mixed with loading buffer (0.3 M Tris, 10% sodium dodecyl sulfate (SDS), 50% vol/vol

glycerol, 3.6 M beta-mercaptoethanol, and 0.5% bromophenol blue), heated at 95°C for 5 min, separated in a 7% SDS-polyacrylamide gel electrophoresis gel, and transferred into a polyvinylidene difluoride (PVDF) membrane (BioRad Laboratories). The PVDF membrane was then incubated with the anti-TSP1 primary antibody (1:1000; R&D systems) at 4°C overnight. After washing, the blot was incubated with anti-goat immunoglobulin conjugated with horseradish peroxidase (1:2000; Zymed Laboratories). Anti-GAPDH antibody (1:5000; Calbiochem) was used as a loading control. The blot image was then visualized by the Pierce SuperSignal West Pico Chemiluminescent substrate (Thermo Fisher Scientific).

2.10 | Outflow facility determination

Adult male C57BL/6J mice (aged 2–4 months old) were used. Ex vivo mouse eyes were continuously perfused with 4-(2-hydroxyethyl)-1-piperazineethanesulfonic acid (HEPES)-buffered Ringer's solution containing either TSP1 blocking or control peptides alone (10 and 50 μM), Y39983 (50 μM) or vehicle (also in the presence of 50 μM blocking/control peptides) throughout the experiments. For perfusions, the anterior chambers of paired mouse eyes were cannulated by a 33-gauge needle. The needle was connected via a pressure transducer (Honeywell) to a glass syringe filled with Ringer's solution at 37°C and placed on a motorized syringe pump (Harvard Apparatus) under computer control. Sequential pressure steps of 4, 8, 12, and 16 mmHg were used. At each pressure step, stable perfusion was obtained for at least 10 min. The measurement of the outflow facility lasted for about 4 h including the equilibration time. The outflow facility was then derived from the average flow rate calculated during the stable perfusion period at each perfusion pressure (Boussommier-Calleja et al., 2012; Lei et al., 2011). All the procedures were approved by the Animal Subjects Ethics Sub-Committee of the Hong Kong Polytechnic University. All experiments were also performed in compliance with the Guide for the Care and Use of Laboratory Animals published by the National Institutes of Health and the ARVO Statement for the Use of Animals in Research.

2.11 | Statistical analysis

Statistical analysis was done with Student's *t*-test or one-way analysis of variance (ANOVA), as appropriate. A $p \leq 0.05$ was considered statistically significant.

3 | RESULTS

3.1 | Effects of Y39983 on morphology, cytoskeletal filamentous actin staining, and motility in hTM cells

Morphology of hTM cells treated for 2 days with different concentrations of Y39983 (0.01, 0.1, and 1 μM) and for vehicle-treated control cells was studied. Stellate cell morphology was observed in hTM cells treated with 1 and 0.1 μM Y39983 (Figure 1a,b) but in neither 0.01 μM Y39983-treated cells nor control (Figure 1c,d).

Treatment of hTM cells for 2 days with 1 μM Y39983 resulted in filamentous actin (F-actin) reorganization, visible after immunostaining, which was absent in the hTM control cells (Figure 2). This F-actin remodeling was observed in Y39983-treated hTM cells, whereas in control cells F-actin remained consistently aligned with stress fiber patterns. In addition, the cell motility assay revealed that Y39983 treatment resulted in a time- and dose-dependent inhibition of hTM cell migration (Figure 3). At 1 μM, Y39983 significantly inhibited the migration of hTM cells to the gap areas, compared with control cells.

3.2 | Effect of Y39983 on TER in hTM cells

Confluent primary hTM cell layers had a net basal TER value of 6.41 kΩ·cm². At 1 μM, Y39983 had no significant effect on the TER (Figure 4). Increasing the concentration of Y39983 to 10 and 50 μM reduced the TER by 25% and 22%, respectively, when compared with the vehicle-treated control ($p \leq 0.05$). In contrast, no significant effect on TM cell viability was observed with Y39983 over a range of concentrations from 0.01 to 50 μM ($p > 0.05$).

3.3 | Protein expression profile of hTM cells after Y39983 treatment using SWATH-MS

A combined IDA proteome library was constructed with a total of 3949 unique, nonredundant proteins derived from 35,449 distinct peptides. Paired comparison of protein abundance was performed to analyze the global protein expression in hTM cells treated with 1 μM Y39983 and vehicle. Biological replicates of hTM cells from three different human donors were used for comparison. After elimination of proteins with fold change below the cutoff level (at ≥1.5 fold) and with only one peptide match in quantitation, 20 proteins with differential expression were identified, including 10 upregulated and 10 downregulated proteins (Table 1). By analyzing these differentially expressed proteins using the online PANTHER classification system, three potential pathways, including the "p53 pathway," "integrin signaling pathway," and "cytoskeletal regulation by Rho GTPase" and four main molecular functions (binding, catalytic activity, transporter activity, and structural molecule activity) were identified (Figure S1).

3.4 | RT-PCR and Western blot analysis for TSP1

TSP1, one of the differentially expressed proteins identified by the proteomic analysis, was selected for further validation by RT-PCR. TSP1 was selected because it was shown to be upregulated in hTM cells by corticosteroids (i.e., compounds known for increasing IOP)
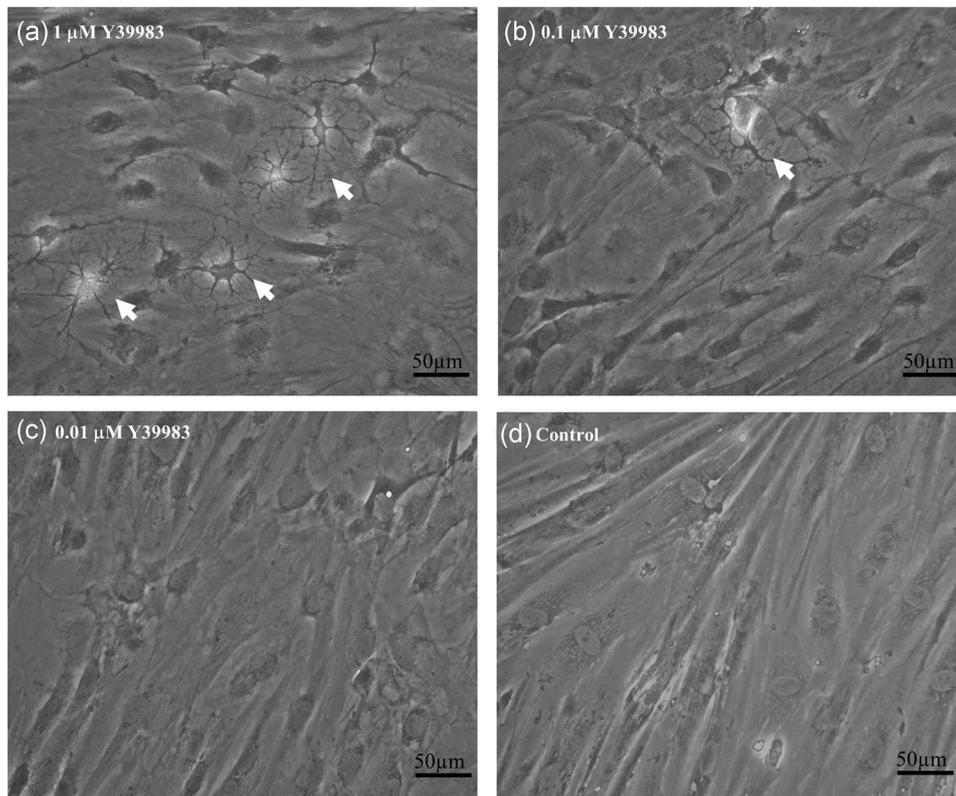
FIGURE 1 Representative phase-contrast microscopy images of hTM cells incubated with (a–c) Y39983 at different concentrations and (d) control for 2 days. Arrows show stellate morphology of hTM cells after treatment at higher concentrations of Y39983. (n = 3). hTM, human TM
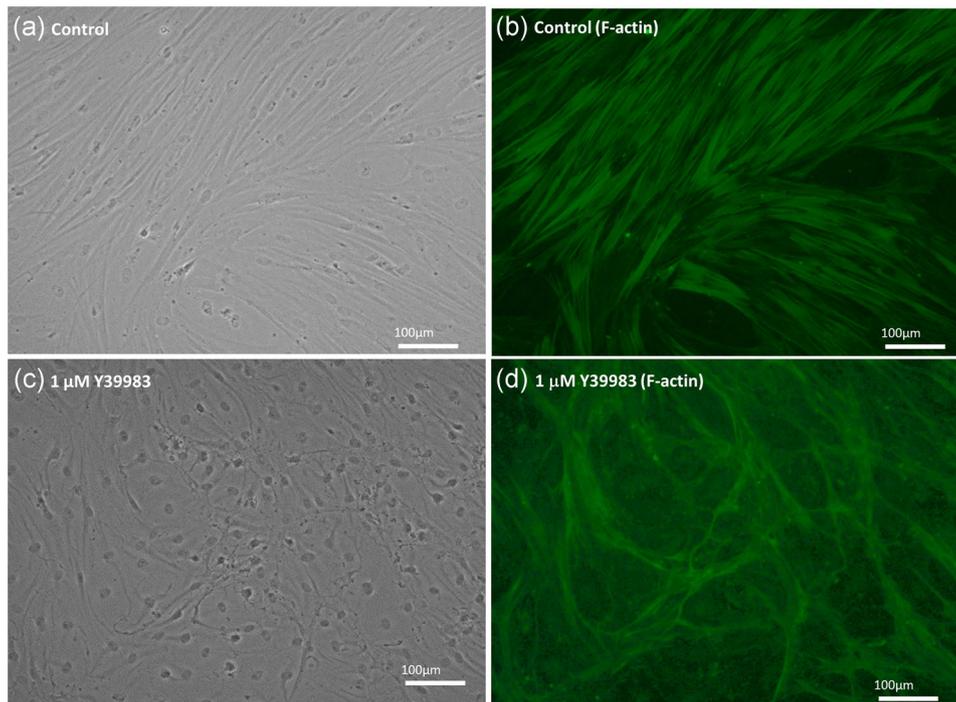

FIGURE 2 Representative phase-contrast and F-actin staining images (equal brightness filtering) of hTM cells treated with (a, b) 1 μM Y39983, and (c, d) control for 2 days, respectively. Stellate-shaped F-actin formations are visible in Y39983-treated hTM cells. (n = 3). hTM, human TM
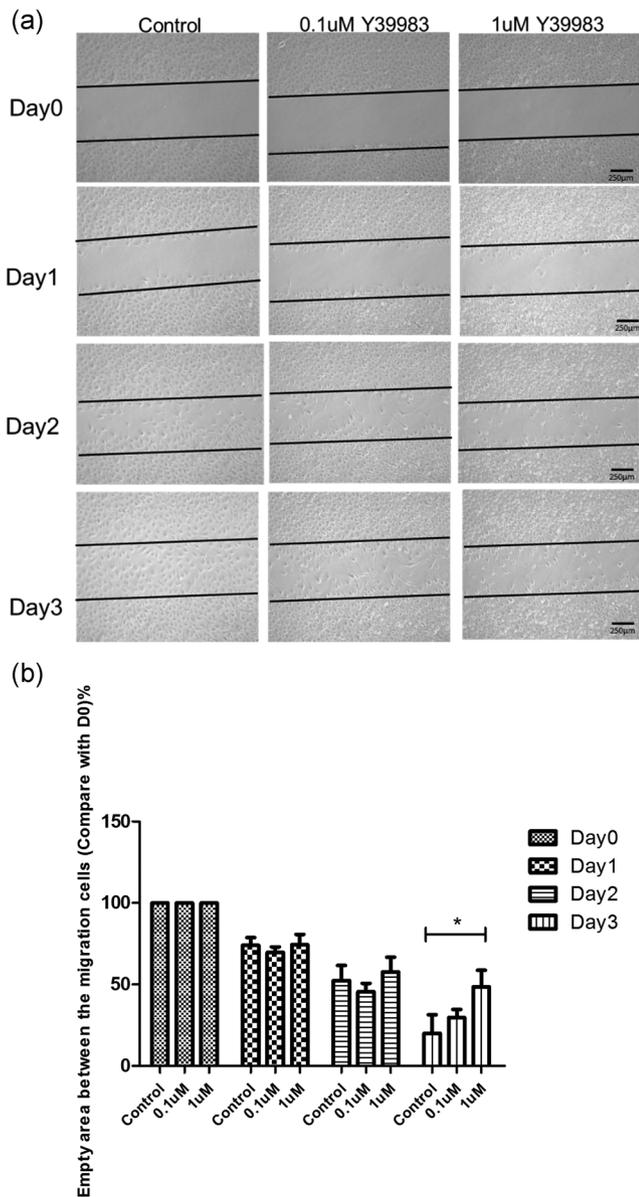
FIGURE 3 Y39983 reduced hTM cell motility. Confluent monolayers were scraped with P20 pipette tips on Day 0, and cell debris was removed by PBS washing, followed by incubation in a fresh medium. (a) Representative photographs of treatment groups at indicated time points. (b) A histogram showing the mean relative empty gap area (measured between the fronts of the migrating cells as compared to Day 0. The data are mean ± SEM ($n = 4$). ANOVA, analysis of variance; hTM, human TM; PBS, phosphate-buffered saline. *$p ≤ 0.05$ (ANOVA)

FIGURE 4 Effect of Y39983 on TER. TER was measured in confluent monolayers of hTM cells grown on Snapwell membrane inserts and treated with different concentrations of Y39983 sequentially (1 h for each concentration) at room temperature. Data represent mean ± *SEM* ($n = 4$); *$p ≤ 0.05$ (ANOVA). ANOVA, analysis of variance; hTM, human TM; TER, transepithelial electrical resistance

3.5 | TSP1 blocking peptide and gene silencing reduced TSP1 expression and cell migration in hTM cells

To investigate the functional relevance of TSP1 in mediating the Y39983-induced effects in hTM cells, the effects of TSP1 antagonist (LSKL, a peptide inhibitor) and gene silencing on TSP1 expression and cell migration were tested. As shown in Figure 6a, LSKL produced a dose-dependent reduction of *TSP1* transcript levels as compared with the control peptide, SLLK, reaching statistical significance at 5 μM. Consistent with the results of LSKL, TSP1 siRNA knockdown produced a dose-dependent suppression of TSP1 transcript levels compared with the negative control siRNA (Figure 6b). In agreement with the gene expression change, TSP1 siRNA (100 pmol) knockdown also suppressed the TSP1 protein level compared with the control siRNA (Figure 6c,d). Similar to Y39983, LSKL suppressed migration of hTM cells, with the effects at 5 μM being more pronounced (Figure 7a), supporting the notion that blocking TSP1 expression reduced hTM cell motility. This was further supported by the suppression of hTM cell migration with TSP1 siRNA knockdown at 100 pmol (Figure 7b).

3.6 | Roles of TSP1 in ROCK-mediated effects on cell migration and outflow facility

To confirm whether the Y39983-induced effects on cell migration and outflow facility were mediated by TSP1 downregulation, hTM cells were coincubated with Y39983 and LSKL simultaneously. As shown in Figures 7c and 7e, there was no difference between

in our previous study (Shan et al., 2017), and TSP1 is also a prominent ECM protein in TM (Flugel-Koch et al., 2004). In this study, TSP1 was downregulated by Y39983, suggesting that TSP1 may play an important role in regulating ROCK inhibitor-mediated increase of outflow facility. Consistent with the SWATH-MS results, *TSP1* transcript levels in hTM cells were reduced by half after Y39983 treatment (Figure 5a). Likewise, TSP1 protein expression was significantly reduced by 80% in Western blot analysis, as shown in Figure 5b,c.
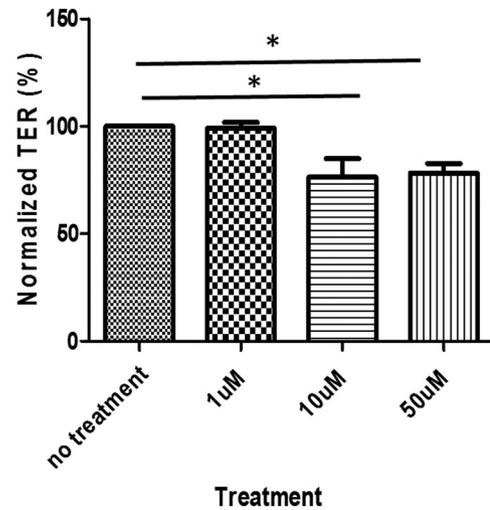
TABLE 1 Identification and fold-change of regulated proteins after Y39983 treatment by SWATH-MS

Protein ID	Uniprot protein accession number	Protein names	Gene ID	Average of log 2 fold changes (Y39983 vs. Ctl)	Average of fold changes (Y39983 vs. Ctl)
1	Q05519	Serine/arginine-rich splicing factor 11	SRSF11	4.49	22.52
2	P23786	Carnitine	CPT2	1.35	2.54
3	O95197	Reticulon-3	RTN3	0.91	1.88
4	Q8TAF3	WD repeat-containing protein 48	WDR48	0.89	1.85
5	Q9NRW3	DNA dC->dU-editing enzyme AP	APOBEC3C	0.86	1.81
6	P08236	Beta-glucuronidase	GUSB	0.53	1.45
7	Q5NDL2	EGF domain-specific	EOGT	0.52	1.43
8	O95218	Zinc finger Ran-binding domain-containing protein 2	ZRANB2	0.48	1.39
9	Q8IWB7	WD repeat and FYVE domain-containing protein 1	WDFY1	0.48	1.39
10	Q08623	Pseudouridine-5'-monophosphatase	PUDP	0.46	1.38
11	P04439	HLA class I histocompatibility antigen, A-3 alpha chain	HLA-A	−0.47	0.72
12	P02452	Collagen alpha-1(I) chain	COL1A1	−0.48	0.72
13	Q5T4S7	E3 ubiquitin-protein ligase UBR4	UBR4	−0.52	0.70
14	P07951	Tropomyosin beta chain	TPM2	−0.52	0.70
15	Q6IAN0	Dehydrogenase/reductase SDR family member 7B	DHRS7B	−0.58	0.67
16	O60610	Protein diaphanous homolog 1	DIAPH1	−0.59	0.66
17	Q9BTZ2	Dehydrogenase/reductase SDR family member 4	DHRS4	−0.63	0.65
18	P07996	Thrombospondin-1	THBS1	−0.73	0.60
19	Q15800	Methylsterol monooxygenase 1	MSMO1	−0.76	0.59
20	Q9Y5B9	FACT complex subunit SPT16	SUPT16H	−1.12	0.46

Note: Green: proteins downregulated by Y39983. Blue: proteins upregulated by Y39983.

Abbreviation: Ctl, control.

Y39983 + LSKL and Y39983 + SLLK, indicating that TSP1 may act through the ROCK pathway. Likewise, coincubation of Y39983 with siRNA-transfected hTM cells did not result in any further suppression of cell migration compared with control scrambled siRNA (Figures 7d and 7f), further supporting the fact that TSP1 may play a pivotal role in mediating the ROCK-induced effects.

As shown in Figure 8a, Y39983 increased the outflow facility in ex vivo mouse eyes by 83.8% compared with the vehicle. In Figure 8b,c, LSKL alone increased the outflow facility in ex vivo mouse eyes by 57.5% at 10 μM and 71.2% at 50 μM, respectively, compared with the respective controls. No significant difference was detected between the effects exerted by Y39983 and LSKL ($p > 0.05$, ANOVA). To confirm whether the effect of Y39983 was mediated by TSP1, the outflow facility was measured after treatment with LSKL and Y39983 simultaneously. When compared with the contralateral eye treated with control peptide SLLK and Y39983 (Figure 8d), no significant difference was detected between the two conditions ($p > 0.05$; $n = 8$).

4 | DISCUSSION

This study demonstrated that Y39983 altered the cytoskeletal structure of hTM cells, and reduced its cell motility and transepithelial resistance, thereby leading to an increase in the outflow facility. Proteomic analysis revealed a downregulation of TSP1 after Y39983 treatment, as confirmed by RT-qPCR and Western blot. LSKL and TSP1 siRNA knockdown reduced TSP1 gene and protein expressions. Likewise, LSKL and TSP1 siRNA treatment retarded hTM cell migration using both cell motility and transwell migration assays. In the presence of Y39983, the effects of LSKL and siRNA knockdown on cell migration were not observed. In addition to in vitro studies, LSKL enhanced the conventional outflow facility in mouse eyes ex vivo, similar to Y39983 alone. No additive effects on outflow facility were detected in mice eyes treated with Y39983 and LSKL simultaneously, suggesting that TSP1 may be an important downstream target for ROCK inhibitor-mediated increase in outflow facility.
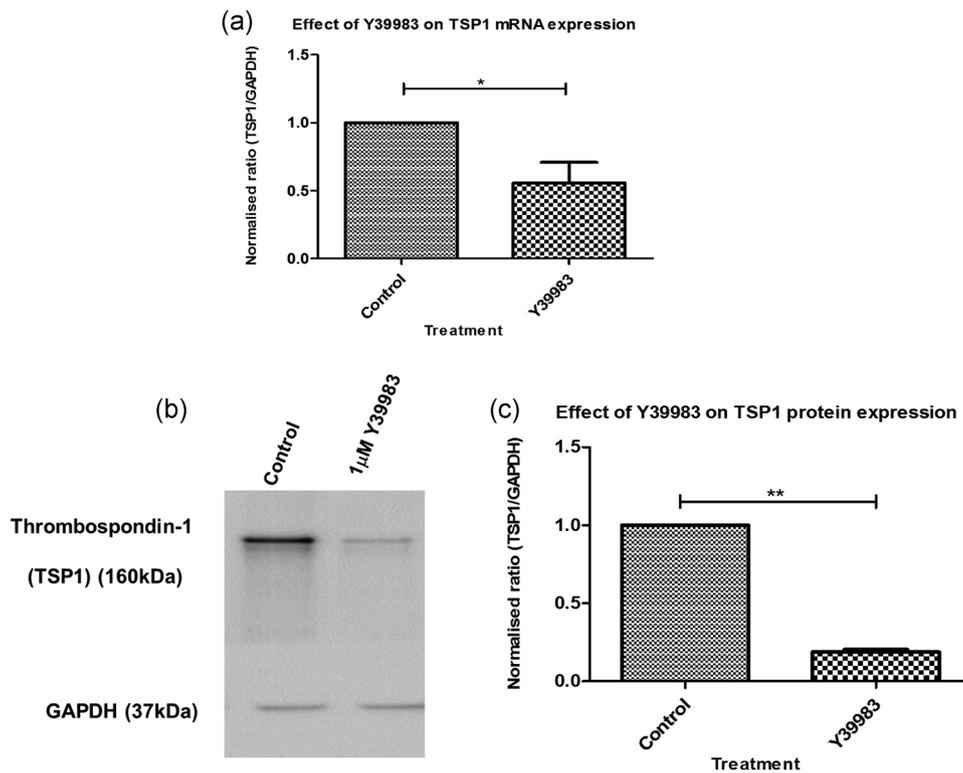
FIGURE 5 Expression of TSP1 mRNA and protein after Y39983 treatment. (a) Effect of Y39983 on TSP1 gene expression in hTM cells by semi-quantitative reverse-transcriptase PCR ($n = 4$; $p \leq 0.05$, Student's t-test). (b) A representative Western blot image showing reduced protein expression of TSP1 after Y39983 treatment for 2 days. (c) Western blot analysis of TSP1 protein expression after Y39983 treatment. The data represent mean ± *SEM* ($n = 4$, $p \leq 0.01$, Student's t-test). hTM, human TM; mRNA, messenger RNA; PCR, polymerase chain reaction; TSP1, thrombospondin-1

Although netarsudil and ripasudil have been approved clinically for glaucoma treatment, other ROCK inhibitors are still under investigation (Kopczynski & Heah, 2018; S. K. Wang & Chang, 2014). Therefore, a better understanding of the underlying cellular mechanisms is crucial in achieving better clinical outcomes. ROCK inhibitors have been shown to alter TM cell morphology and migration, actin stress fibers, and focal adhesions (Rao et al., 2001, 2005). In addition, they have been shown to increase SC cell monolayer permeability with disrupted tight junctions (Kameda et al., 2012; Kaneko et al., 2016). In this study, our primary aim was to evaluate the potential significance of TSP1 in regulating ROCK inhibitor-mediated responses in TM cells. Y39983 was selected because it is a potent inhibitor. It has been shown that Y39983 has a stronger effect than other ROCK inhibitors in promoting neurite outgrowth of retinal ganglion cells (Lingor et al., 2008), making it more appealing to glaucoma therapy because of its potential IOP-lowering and neuroprotective properties. The actin cytoskeleton is known to interact with ECM receptors, such as integrins, to regulate cell shape and cell adhesion to the ECM. Our results showed that Y39983 altered cytoskeletal protein rearrangement by reducing actin stress fibers in TM cells, potentially widening intracellular spaces in the TM (K. Wang et al., 2017). To determine whether the observed morphological and structural changes affecting cell function and behavior, the effects of Y39983 on hTM cell motility and transepithelial

resistance were studied. The findings of the cell migration assay showed that the alteration of actin stress fibers by Y39983 limited the TM cell motility. Concomitantly, Y39983 triggered a reduction of TER in cultured hTM cell layers, reflecting an altered paracellular pathway governed by tight junctions and cell–cell interactions (Meyle et al., 1999). Our results are in agreement with the findings reported in monkey SC cells, in which the endothelial cell permeability was reduced by K-115 (Kaneko et al., 2016).

The differential protein expression profile of hTM cells was investigated after Y39983 treatment. Of the 20 proteins with significantly altered expression, pathway analysis revealed the involvement of three major pathways: the "p53 pathway," "cytoskeletal pathway regulation by Rho GTPase," and "integrin signaling pathway." As evidence by genetic linkage studies, we have identified a number of differentially expressed proteins that are associated with the pathogenesis of glaucoma. For example, the tropomyosin beta chain, which is an actin-binding protein that plays an important role in regulating muscle contraction (Prabhakar et al., 1999), has been reported to be upregulated in the TM of glaucomatous patients (Fatma et al., 2009; Zhao et al., 2004). We show that Y39983 reduces the expression of the tropomyosin beta chain, suggesting that Y39983 may exert its IOP-lowering effect by influencing the coordination of cytoskeletal structures in hTM cells. Similarly, down-regulation of collagen type I alpha 1 chain (COL1A1) was observed
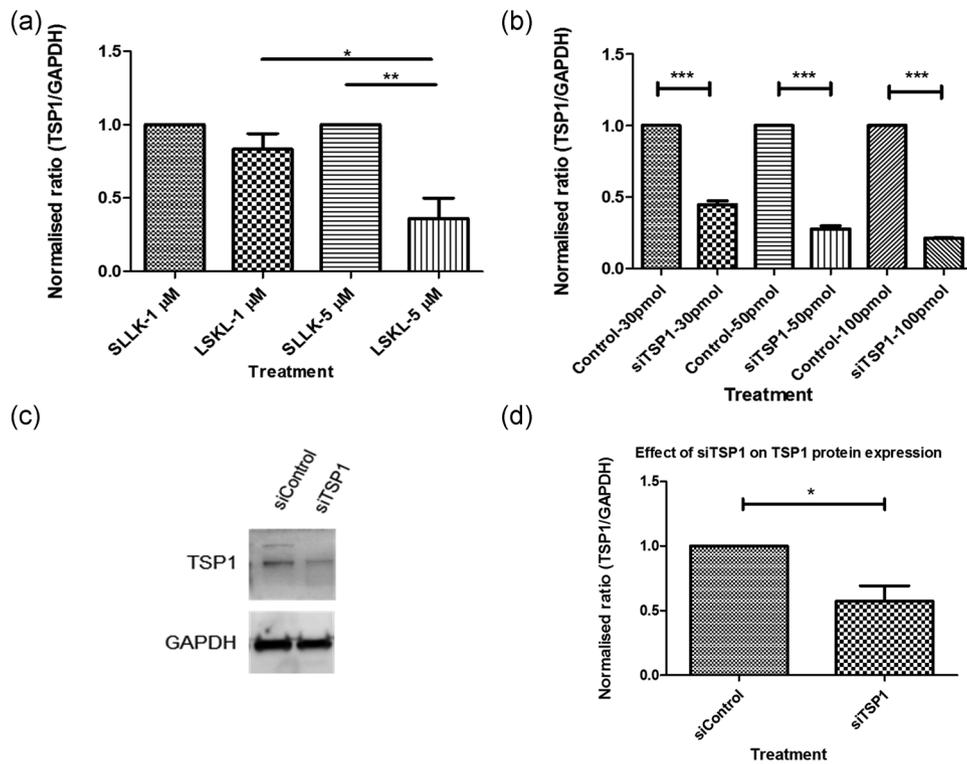
FIGURE 6 Quantification of TSP1 gene expression by quantitative real-time PCR. (a) hTM cells treated with TSP1 blocking peptide (LSKL) or control peptide (SLLK) (at 1 and 5 μM) for 2 days (n = 5 per group). (b) TSP1 siRNA and scrambled control siRNA were transfected for 24 h (n = 3 per group). (c, d) Western blot analysis of TSP1 protein expression in hTM cells after siRNA treatment for 24 h (n = 3). The data represent mean ± *SEM* *$p \leq 0.05$; **$p \leq 0.01$ ***$p \leq 0.001$ (Student's *t*-test). hTM, human TM; LSKL, leucine–serine–lysine–leucine; PCR, polymerase chain reaction; siRNA, small interfering RNA; SLLK, serine–leucine–leucine–lysine; TSP1, thrombospondin-1

following Y39983 treatment, as demonstrated by the identification of integrin pathway in the pathway analyses. It has been reported that *COL1A1* mutations occur in different forms of glaucoma (Mauri et al., 2016). Transgenic *Col1a1*^r/r mice have been shown to display an elevated IOP with a reduced outflow facility (Dai et al., 2009). Overexpressing *Col1a1*^r/r is found to increase ECM deposition in the outflow pathway, leading to a raised IOP in mice (Aihara et al., 2003). In addition, our results reveal an increase in beta-glucuronidase expression after Y39983 treatment. Beta-glucuronidase is an enzyme promoting degradation of GAGs (Meyerrose et al., 2008). Application of an inhibitor of hyaluronan (HA) and HA-short hairpin RNA silencing lentivirus has been shown to increase the outflow facility in porcine eyes (Keller et al., 2012).

To the best of our knowledge, this study is the first to demonstrate the downregulation of TSP1 after ROCK inhibition. TSP1 is a multifunctional matricellular ECM protein and has numerous biological functions including cell migration, cell adhesion, and regulation of growth factors (e.g., fibroblast growth factor, vascular endothelial growth factor, and epidermal growth factor; Adams & Lawler, 2011). TSP1 has been implicated in glaucoma pathology (Flugel-Koch et al., 2004; Overby et al., 2014) as it is an activator of TGF-β (Murphy-Ullrich et al., 1992), and increases the expression of TGF-β in the plasma of patients with POAG (Kuchtey et al., 2014). In addition, the expression of TSP1 is found to increase in glaucomatous eyes (Flugel-

Koch et al., 2004). Recently, we have also demonstrated that expression of TSP1 in hTM cells is increased after dexamethasone treatment, a known risk factor for increased IOP and glaucoma (Shan et al., 2017). Our results show that Y39983 downregulates the expression of the TSP1 gene and protein simultaneously. Although Y39983 downregulates TSP1 gene expression by 50%, it reduces the protein expression by ~80%. This difference could be due to protein degradation, shorter protein half-life, and other posttranscriptional mechanisms. Consistent with the results obtained from Y39983, LSKL inhibited TSP1 gene and protein expressions, as well as hTM cell migration. As LSKL peptide acts as a competitive TGF-β antagonist, our results might suggest that the inhibitory effects of LSKL on TSP1 expression and hTM cell migration are secondary due to reduction in active TGF-β (Broekelmann et al., 2020). Nevertheless, our findings of TSP1 siRNA knockdown provide direct evidence of TSP1 involvement in regulating TM cell migration. In the presence of Y39983, the inhibition of cell migration by LSKL and siRNA knockdown was not observed (Figure 7c–f), strongly indicating that TSP1 may be an important downstream target for ROCK inhibition. Together with the observed changes in TER and F-actin network, it is likely that TM cell migration is mediated by ECM remodeling and cell–matrix interactions (Koudouna et al., 2020), as TSP1 has been shown to inhibit matrix metallopeptidase activities (Adams & Lawler, 2011; Bornstein et al., 2004; Calabro
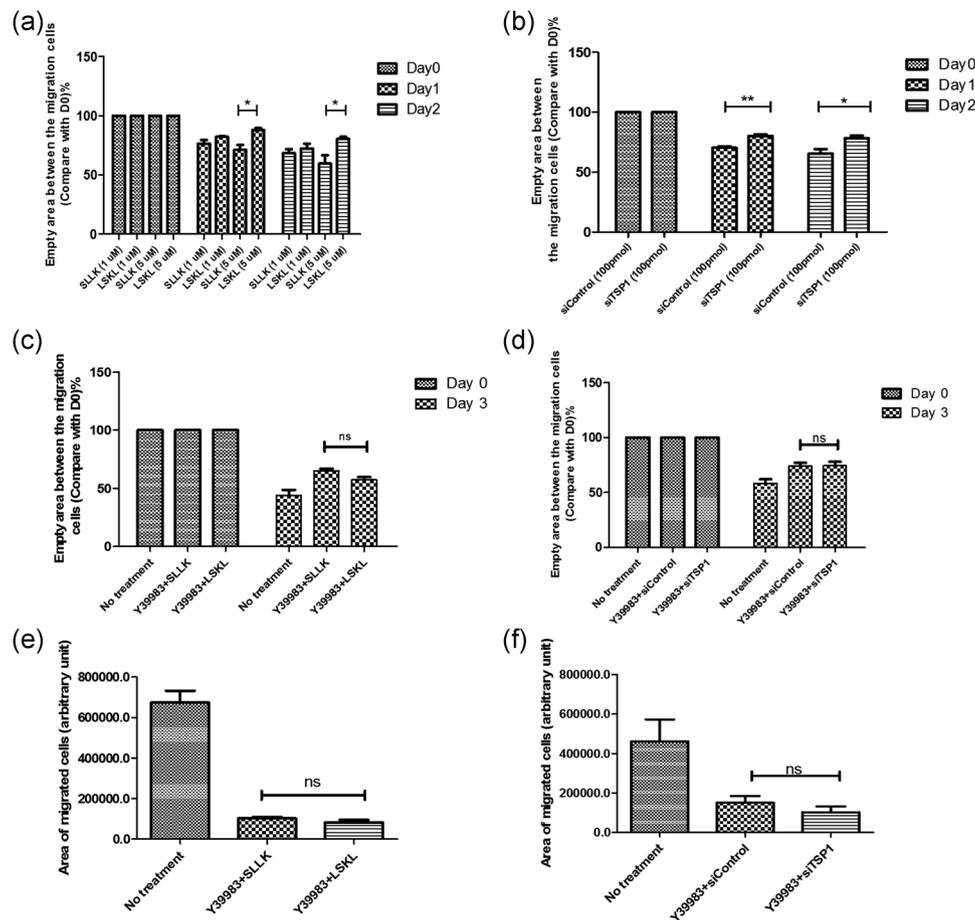
FIGURE 7 Cell motility assays showing the effects of TSP1 inhibitor and siRNA knockdown. Gap opening area is presented as a percentage of Day 0 gap width. (a) Treatment of LSKL or SLLK at different concentrations ($n = 3$ per group). (b) Transfection with TSP1 siRNA and NC scrambled control siRNA ($n = 3$ per group). (c) Treatment of 1 µM Y39983 combined with 5 µM of LSKL or SLLK ($n = 4$ per group). (d) Treatment of 1 µM Y39983 combined with 100 pmol of control or TSP1 siRNA ($n = 4$ per group). (e) Transwell migration in treatment of 1 µM Y39983 combined with 5 µM of LSKL or SLLK for 2 days ($n = 3$ per group). (f) Transwell migration in treatment of 1 µM Y39983 combined with 100 pmol of control or TSP1 siRNA for 2 days ($n = 3$ per group). SLLK: control peptide; LSKL: TSP1 blocking peptide. The data represent mean ± *SEM*. LSKL, leucine–serine–lysine–leucine; NC, negative control; ns, not statistically significant; siRNA, small interfering RNA; SLLK, serine–leucine–leucine–lysine; TSP1, thrombospondin-1. **$p \leq 0.01$; *$p \leq 0.05$ (Student's *t*-test)

et al., 2014). The functional relevance of TSP1 downregulation was further confirmed by the direct effect of LSKL on the outflow facility. Both LSKL and Y39983 increased the outflow facility to a similar extent. No additive effect was observed in combining LSKL with Y39983, supporting the notion that effects exerted by Y39983 may be mediated by TSP1. These results are consistent with the previous findings that TSP1-null mice displayed a reduced IOP (Haddadin et al., 2012; Wallace et al., 2014). Despite that, we cannot rule out the possibility that TSP1 may have affected other cell types such as SC cells, as ROCK inhibitor was shown to influence its permeability and outflow resistance (Kameda et al., 2012; Kaneko et al., 2016). Very recently, it has been demonstrated that the expression of *THBS1* is significantly higher in the TM compared to the SC (Patel et al., 2020; van Zyl et al., 2020).

In addition, a correlation between TSP1 and the p53 pathway has been reported in various tumor cell types, including bladder cancer, prostate cancer, and renal cell carcinoma (Giuriato et al., 2006). The p53 pathway contains a network of genes, the products of which are targeted to different intrinsic and extrinsic stress signals, thereby regulating DNA repair processes, cell division, and genome stability (Vogelstein et al., 2000). It has been shown that TSP1 is activated by the p53 pathway (L. Zhang et al., 2000) and is downregulated by p53-induced microRNA-194 (Sundaram et al., 2011), potentially influencing cell to cell communication by modifying both the cellular and ECM environment.

Taken together, the findings of cytoskeletal remodeling along with reduced cell migration and tissue resistance provided a better understanding of the cellular events induced by ROCK inhibition in hTM cells. In addition, we revealed that ROCK inhibitor-induced cytoskeletal changes may alter ECM synthesis and expression in hTM cells. This interplay between cytoskeletal remodeling and ECM synthesis in TM cells represents an important regulatory mechanism in the modulation of outflow resistance (Pattabiraman & Rao, 2010). This study provides the first evidence for reduced TSP1 expression as a potential downstream target in ROCK inhibition. Considering that TSP1 is upregulated in
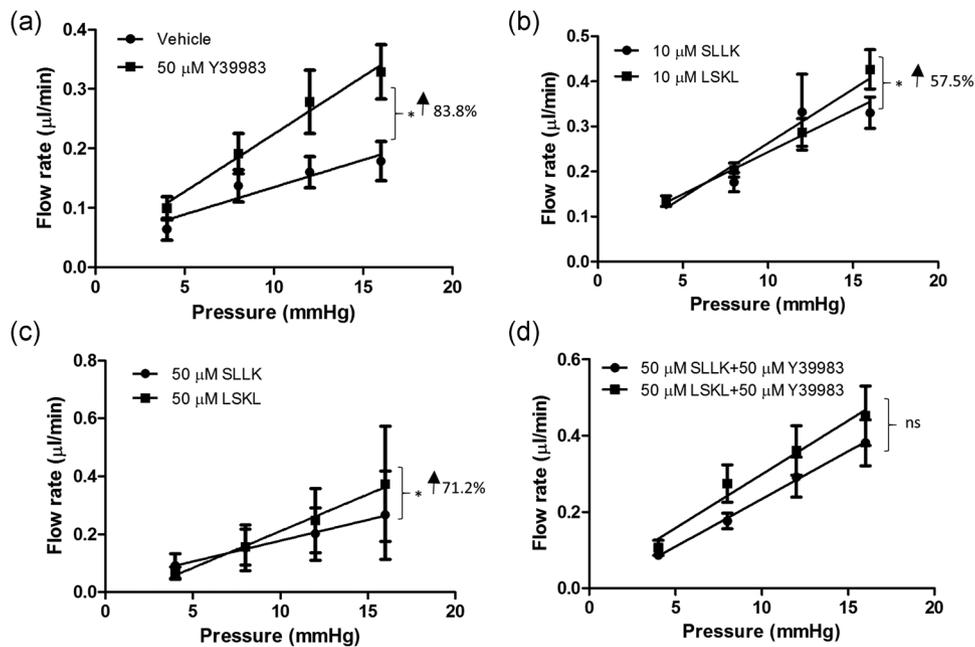
FIGURE 8 Outflow facility in enucleated eyes from C57BL/6J mice. Measurements of flow rate in paired mouse eyes in the presence of (a) 50 μM Y39983 or control vehicle ($n = 6$); (b) TSP1 blocking peptide (10 μM LSKL) or control peptide (10 μM SLLK) ($n = 8$); (c) TSP1 blocking peptide (50 μM LSKL) or control peptide (50 μM SLLK) ($n = 6$); (d) 50 μM LSKL or SLLK with 50 μM Y39983 ($n = 8$). Data are shown as mean ± SEM; ns; *$p ≤ 0.05$ (Student's t-test). LSKL, leucine–serine–lysine–leucine; ns, not statistically significant; SLLK, serine–leucine–leucine–lysine; TSP1, thrombospondin-1

glaucomatous eyes and TSP1 genetic ablation lowers IOP, our results suggest that TSP1, via ROCK inhibition, represents a potential therapeutic target for enhancing outflow facility.

CONFLICT OF INTERESTS

The authors declare that there are no conflict of interests.

DATA AVAILABILITY STATEMENT

The data that support the findings of this study are openly available in (Peptide Atlas public repository) at http://www.peptideatlas.org/, reference number (Data ID PASS01254).

REFERENCES

Adams, J. C., & Lawler, J. (2011). The thrombospondins. *Cold Spring Harbor Perspectives in Biology*, 3(10), a009712. https://doi.org/10.1101/cshperspect.a009712

Aihara, M., Lindsey, J. D., & Weinreb, R. N. (2003). Ocular hypertension in mice with a targeted type I collagen mutation. *Investigative Ophthalmology and Visual Science*, 44(4), 1581–1585. https://doi.org/10.1167/iovs.02-0759

Alvarado, J. A., Yun, A. J., & Murphy, C. G. (1986). Juxtacanalicular tissue in primary open angle glaucoma and in nonglaucomatous normals. *Archives of Ophthalmology*, 104(10), 1517–1528.

Belmadani, S., Bernal, J., Wei, C. C., Pallero, M. A., Dell'italia, L., Murphy-Ullrich, J. E., & Berecek, K. H. (2007). A thrombospondin-1 antagonist of transforming growth factor-beta activation blocks cardiomyopathy in rats with diabetes and elevated angiotensin II. *American Journal of Pathology*, 171(3), 777–789. https://doi.org/10.2353/ajpath.2007.070056

Bill, A., & Phillips, C. I. (1971). Uveoscleral drainage of aqueous humour in human eyes. *Experimental Eye Research*, 12(3), 275–281.

Bornstein, P., Agah, A., & Kyriakides, T. R. (2004). The role of thrombospondins 1 and 2 in the regulation of cell-matrix interactions, collagen fibril formation, and the response to injury. *International Journal of Biochemistry and Cell Biology*, 36(6), 1115–1125. https://doi.org/10.1016/j.biocel.2004.01.012

Boussommier-Calleja, A., Bertrand, J., Woodward, D. F., Ethier, C. R., Stamer, W. D., & Overby, D. R. (2012). Pharmacologic manipulation of conventional outflow facility in ex vivo mouse eyes. *Investigative Ophthalmology and Visual Science*, 53(9), 5838–5845. https://doi.org/10.1167/iovs.12-9923

Broekelmann, T. J., Bodmer, N. K., & Mecham, R. P. (2020). Identification of the growth factor-binding sequence in the extracellular matrix protein MAGP-1. *Journal of Biological Chemistry*, 295(9), 2687–2697. https://doi.org/10.1074/jbc.RA119.010540

Calabro, N. E., Kristofik, N. J., & Kyriakides, T. R. (2014). Thrombospondin-2 and extracellular matrix assembly. *Biochimica et Biophysica Acta/General Subjects*, 1840(8), 2396–2402. https://doi.org/10.1016/j.bbagen.2014.01.013

Chen, Y., Yan, H., Li, G., & Zhang, Y. (2020). Higher TGF-beta1, TGF-beta2, MMP-2 and TIMP-1 Levels in the aqueous humor of the patients with acute primary angle closure. _Ophthalmic Research_, 64, 62–67. https://doi.org/10.1159/000507762

Cheng, A. K., Civan, M. M., To, C. H., & Do, C. W. (2016). cAMP stimulates transepithelial short-circuit current and fluid transport across porcine ciliary epithelium. _Investigative Ophthalmology and Visual Science_, 57(15), 6784–6794. https://doi.org/10.1167/iovs.16-20127

Dai, Y., Lindsey, J. D., Duong-Polk, X., Nguyen, D., Hofer, A., & Weinreb, R. N. (2009). Outflow facility in mice with a targeted type I collagen mutation. _Investigative Ophthalmology and Visual Science_, 50(12), 5749–5753. https://doi.org/10.1167/iovs.08-3367

Dang, Y., Wang, C., Shah, P., Waxman, S., Loewen, R. T., & Loewen, N. A. (2019). RKI-1447, a Rho kinase inhibitor, causes ocular hypotension, actin stress fiber disruption, and increased phagocytosis. _Graefes Archive for Clinical and Experimental Ophthalmology_, 257(1), 101–109. https://doi.org/10.1007/s00417-018-4175-6

Fatma, N., Kubo, E., Toris, C. B., Stamer, W. D., Camras, C. B., & Singh, D. P. (2009). PRDX6 attenuates oxidative stress- and TGFbeta-induced abnormalities of human trabecular meshwork cells. _Free Radical Research_, 43(9), 783–795. https://doi.org/10.1080/10715760903062887

Flugel-Koch, C., Ohlmann, A., Fuchshofer, R., Welge-Lussen, U., & Tamm, E. R. (2004). Thrombospondin-1 in the trabecular meshwork: Localization in normal and glaucomatous eyes, and induction by TGF-beta1 and dexamethasone in vitro. _Experimental Eye Research_, 79(5), 649–663. https://doi.org/10.1016/j.exer.2004.07.005

Fuchshofer, R., & Tamm, E. R. (2012). The role of TGF-beta in the pathogenesis of primary open-angle glaucoma. _Cell and Tissue Research_, 347(1), 279–290. https://doi.org/10.1007/s00441-011-1274-7

Fukata, Y., Amano, M., & Kaibuchi, K. (2001). Rho-Rho-kinase pathway in smooth muscle contraction and cytoskeletal reorganization of non-muscle cells. _Trends In Pharmacological Sciences_, 22(1), 32–39.

Garnock-Jones, K. P. (2014). Ripasudil: First global approval. _Drugs_, 74(18), 2211–2215. https://doi.org/10.1007/s40265-014-0333-2

Giuriato, S., Ryeom, S., Fan, A. C., Bachireddy, P., Lynch, R. C., Rioth, M. J., van Riggelen, J., Kopelman, A. M., Passegué, E., Tang, F., Folkman, J., & Felsher, D. W. (2006). Sustained regression of tumors upon MYC inactivation requires p53 or thrombospondin-1 to reverse the angiogenic switch. _Proceedings of the National Academy of Sciences of the United States of America_, 103(44), 16266–16271. https://doi.org/10.1073/pnas.0608017103

Haddadin, R. I., Oh, D. J., Kang, M. H., Villarreal, G., Jr., Kang, J. H., Jin, R., Gong, H., & Rhee, D. J. (2012). Thrombospondin-1 (TSP1)-null and TSP2-null mice exhibit lower intraocular pressures. _Investigative Ophthalmology and Visual Science_, 53(10), 6708–6717. https://doi.org/10.1167/iovs.11-9013

Honjo, M., Tanihara, H., Inatani, M., Kido, N., Sawamura, T., Yue, B. Y., Narumiya, S., & Honda, Y. (2001). Effects of Rho-associated protein kinase inhibitor Y-27632 on intraocular pressure and outflow facility. _Investigative Ophthalmology and Visual Science_, 42(1), 137–144.

Inatani, M., Tanihara, H., Katsuta, H., Honjo, M., Kido, N., & Honda, Y. (2001). Transforming growth factor-beta 2 levels in aqueous humor of glaucomatous eyes. _Graefes Archive for Clinical and Experimental Ophthalmology_, 239(2), 109–113. https://doi.org/10.1007/s004170000241

Jocson, V. L., & Sears, M. L. (1971). Experimental aqueous perfusion in enucleated human eyes. Results after obstruction of Schlemm's canal. _Archives of Ophthalmology_, 86(1), 65–71. https://doi.org/10.1001/archopht.1971.01000010067013

Kaibuchi, K., Kuroda, S., & Amano, M. (1999). Regulation of the cytoskeleton and cell adhesion by the Rho family GTPases in mammalian cells. _Annual Review of Biochemistry_, 68, 459–486. https://doi.org/10.1146/annurev.biochem.68.1.459

Kameda, T., Inoue, T., Inatani, M., Fujimoto, T., Honjo, M., Kasaoka, N., Inoue-Mochita, M., Yoshimura, N., & Tanihara, H. (2012). The effect of Rho-associated protein kinase inhibitor on monkey Schlemm's canal endothelial cells. _Investigative Ophthalmology and Visual Science_, 53(6), 3092–3103. https://doi.org/10.1167/iovs.11-8018

Kaneko, Y., Ohta, M., Inoue, T., Mizuno, K., Isobe, T., Tanabe, S., & Tanihara, H. (2016). Effects of K-115 (Ripasudil), a novel ROCK inhibitor, on trabecular meshwork and Schlemm's canal endothelial cells. _Scientific Reports_, 6, 19640. https://doi.org/10.1038/srep19640

Keller, K. E., Bhattacharya, S. K., Borrás, T., Brunner, T. M., Chansangpetch, S., Clark, A. F., Dismuke, W. M., Du, Y., Elliott, M. H., Ethier, C. R., Faralli, J. A., Freddo, T. F., Fuchshofer, R., Giovingo, M., Gong, H., Gonzalez, P., Huang, A., Johnstone, M. A., Kaufman, P. L., … Stamer, W. D. (2018). Consensus recommendations for trabecular meshwork cell isolation, characterization and culture. _Experimental Eye Research_, 171, 164–173. https://doi.org/10.1016/j.exer.2018.03.001

Keller, K. E., Sun, Y. Y., Yang, Y. F., Bradley, J. M., & Acott, T. S. (2012). Perturbation of hyaluronan synthesis in the trabecular meshwork and the effects on outflow facility. _Investigative Ophthalmology and Visual Science_, 53(8), 4616–4625. https://doi.org/10.1167/iovs.12-9500

Kopczynski, C. C., & Heah, T. (2018). Netarsudil ophthalmic solution 0.02% for the treatment of patients with open-angle glaucoma or ocular hypertension, _Drugs Today_, 54(8), 467-478. https://doi.org/10.1358/dot.2018.54.8.2849627

Koudouna, E., Spurlin, J., Babushkina, A., Quantock, A. J., Jester, J. V., & Lwigale, P. (2020). Recapitulation of normal collagen architecture in embryonic wounded corneas. _Scientific Reports_, 10(1), 13815. https://doi.org/10.1038/s41598-020-70658-y

Kuchtey, J., Kunkel, J., Burgess, L. G., Parks, M. B., Brantley, M. A., Jr., & Kuchtey, R. W. (2014). Elevated transforming growth factor beta1 in plasma of primary open-angle glaucoma patients. _Investigative Ophthalmology and Visual Science_, 55(8), 5291–5297. https://doi.org/10.1167/iovs.14-14578

Lei, Y., Overby, D. R., Boussommier-Calleja, A., Stamer, W. D., & Ethier, C. R. (2011). Outflow physiology of the mouse eye: Pressure dependence and washout. _Investigative Ophthalmology and Visual Science_, 52(3), 1865–1871. https://doi.org/10.1167/iovs.10-6019

Li, S. K., Shan, S. W., Li, H. L., Cheng, A. K., Pan, F., Yip, S. P., Civan, M. M., To, C. H., & Do, C. W. (2018). Characterization and regulation of gap junctions in porcine ciliary epithelium. _Investigative Ophthalmology and Visual Science_, 59(8), 3461–3468. https://doi.org/10.1167/iovs.18-24682

Lingor, P., Tonges, L., Pieper, N., Bermel, C., Barski, E., Planchamp, V., & Bahr, M. (2008). ROCK inhibition and CNTF interact on intrinsic signalling pathways and differentially regulate survival and regeneration in retinal ganglion cells. _Brain_, 131(Pt 1), 250–263. https://doi.org/10.1093/brain/awm284

Mauri, L, Uebe, S., Sticht, H., Vossmerbaeumer, U., Weisschuh, N., Manfredini, E., Maselli, E., Patrosso, M., Weinreb, R. N., Penco, S., Reis, A., & Pasutto, F. (2016). Expanding the clinical spectrum of COL1A1 mutations in different forms of glaucoma. _Orphanet Journal of Rare Diseases_, 11(1), 108. https://doi.org/10.1186/s13023-016-0495-y

Mehran, N. A., Sinha, S., & Razeghinejad, R. (2020). New glaucoma medications: Latanoprostene bunod, netarsudil, and fixed combination netarsudil-latanoprost. _Eye_, 34(1), 72–88. https://doi.org/10.1038/s41433-019-0671-0

Meyerrose, T. E., Roberts, M., Ohlemiller, K. K., Vogler, C. A., Wirthlin, L., Nolta, J. A., & Sands, M. S. (2008). Lentiviral-transduced human mesenchymal stem cells persistently express therapeutic levels of enzyme in a xenotransplantation model of human disease. _Stem Cells_, 26(7), 1713–1722. https://doi.org/10.1634/stemcells.2008-0008

Meyle, J., Gultig, K., Rascher, G., & Wolburg, H. (1999). Transepithelial electrical resistance and tight junctions of human gingival keratinocytes. *Journal of Periodontal Research*, 34(4), 214–222. https://doi.org/10.1111/j.1600-0765.1999.tb02244.x

Murphy-Ullrich, J. E., Schultz-Cherry, S., & Hook, M. (1992). Transforming growth factor-beta complexes with thrombospondin. *Molecular Biology of the Cell*, 3(2), 181–188. https://doi.org/10.1091/mbc.3.2.181

Nobes, C. D., & Hall, A. (1995). Rho, rac and cdc42 GTPases: Regulators of actin structures, cell adhesion and motility. *Biochemical Society Transactions*, 23(3), 456–459.

Overby, D. R., Zhou, E. H., Vargas-Pinto, R., Pedrigi, R. M., Fuchshofer, R., Braakman, S. T., Gupta, R., Perkumas, K. M., Sherwood, J. M., Vahabikashi, A., Dang, Q., Kim, J. H., Ethier, C. R., Stamer, W. D., Fredberg, J. J., & Johnson, M. (2014). Altered mechanobiology of Schlemm's canal endothelial cells in glaucoma. *Proceedings of the National Academy of Sciences of the United States of America*, 111(38), 13876–13881. https://doi.org/10.1073/pnas.1410602111

Patel, G., Fury, W., Yang, H., Gomez-Caraballo, M., Bai, Y., Yang, T., Adler, C., Wei, Y., Ni, M., Schmitt, H., Hu, Y., Yancopoulos, G., Stamer, W. D., & Romano, C. (2020). Molecular taxonomy of human ocular outflow tissues defined by single-cell transcriptomics. *Proceedings of the National Academy of Sciences of the United States of America*, 117(23), 12856–12867. https://doi.org/10.1073/pnas.2001896117

Pattabiraman, P. P., & Rao, P. V. (2010). Mechanistic basis of Rho GTPase-induced extracellular matrix synthesis in trabecular meshwork cells. *American Journal of Physiology: Cell Physiology*, 298(3), C749–C763. https://doi.org/10.1152/ajpcell.00317.2009

Prabhakar, R., Boivin, G. P., Hoit, B., & Wieczorek, D. F. (1999). Rescue of high expression beta-tropomyosin transgenic mice by 5-propyl-2-thiouracil. Regulating the alpha-myosin heavy chain promoter. *Journal of Biological Chemistry*, 274(41), 29558–29563.

Rao, P. V., Deng, P., Sasaki, Y., & Epstein, D. L. (2005). Regulation of myosin light chain phosphorylation in the trabecular meshwork: Role in aqueous humour outflow facility. *Experimental Eye Research*, 80(2), 197–206. https://doi.org/10.1016/j.exer.2004.08.029

Rao, P. V., Deng, P. F., Kumar, J., & Epstein, D. L. (2001). Modulation of aqueous humor outflow facility by the Rho kinase-specific inhibitor Y-27632. *Investigative Ophthalmology and Visual Science*, 42(5), 1029–1037.

Rohen, J. W. (1983). Why is intraocular pressure elevated in chronic simple glaucoma? Anatomical considerations. *Ophthalmology*, 90(7), 758–765.

Shan, S. W., Do, C. W., Lam, T. C., Kong, R., Li, K. K., Chun, K. M., Stamer, W. D., & To, C. H. (2017). New insight of common regulatory pathways in human trabecular meshwork cells in response to dexamethasone and prednisolone using an integrated quantitative proteomics: SWATH and MRM-HR mass spectrometry. *Journal of Proteome Research*, 16(10), 3753–3765. https://doi.org/10.1021/acs.jproteome.7b00449

Shan, S. W., Do, C. W., Lam, T. C., Li, H. L., Daniel Stamer, W., & To, C. H. (2020). Data on differentially expressed proteins in rock inhibitor-treated human trabecular meshwork cells using SWATH-based proteomics. *Data in Brief*, 31, 105846. https://doi.org/10.1016/j.dib.2020.105846

Shan, S. W., Lee, D. Y., Deng, Z., Shatseva, T., Jeyapalan, Z., Du, W. W., Zhang, Y., Xuan, J. W., Yee, S. P., Siragam, V., & Yang, B. B. (2009). MicroRNA MiR-17 retards tissue growth and represses fibronectin expression. *Nature Cell Biology*, 11(8), 1031–1038. https://doi.org/10.1038/ncb1917

Snyder, R. W., Stamer, W. D., Kramer, T. R., & Seftor, R. E. (1993). Corticosteroid treatment and trabecular meshwork proteases in cell and organ culture supernatants. *Experimental Eye Research*, 57(4), 461–468.

Stamer, W. D., Seftor, R. E., Williams, S. K., Samaha, H. A., & Snyder, R. W. (1995). Isolation and culture of human trabecular meshwork cells by extracellular matrix digestion. *Current Eye Research*, 14(7), 611–617.

Sundaram, P., Hultine, S., Smith, L. M., Dews, M., Fox, J. L., Biyashev, D., Schelter, J. M., Huang, Q., Cleary, M. A., Volpert, O. V., & Thomas-Tikhonenko, A. (2011). p53-responsive miR-194 inhibits thrombospondin-1 and promotes angiogenesis in colon cancers. *Cancer Research*, 71(24), 7490–7501. https://doi.org/10.1158/0008-5472.CAN-11-1124

Tokushige, H., Inatani, M., Nemoto, S., Sakaki, H., Katayama, K., Uehata, M., & Tanihara, H. (2007). Effects of topical administration of y-39983, a selective Rho-associated protein kinase inhibitor, on ocular tissues in rabbits and monkeys. *Investigative Ophthalmology and Visual Science*, 48(7), 3216–3222. https://doi.org/10.1167/iovs.05-1617

van Zyl, T., Yan, W., McAdams, A., Peng, Y. R., Shekhar, K., Regev, A., Juric, D., & Sanes, J. R. (2020). Cell atlas of aqueous humor outflow pathways in eyes of humans and four model species provides insight into glaucoma pathogenesis. *Proceedings of the National Academy of Sciences of the United States of America*, 117(19), 10339–10349. https://doi.org/10.1073/pnas.2001250117

Vogelstein, B., Lane, D., & Levine, A. J. (2000). Surfing the p53 network. *Nature*, 408(6810), 307–310. https://doi.org/10.1038/35042675

Wallace, D. M., Murphy-Ullrich, J. E., Downs, J. C., & O'Brien, C. J. (2014). The role of matricellular proteins in glaucoma. *Matrix Biology*, 37, 174–182. https://doi.org/10.1016/j.matbio.2014.03.007

Wang, K., Read, A. T., Sulchek, T., & Ethier, C. R. (2017). Trabecular meshwork stiffness in glaucoma. *Experimental Eye Research*, 158, 3–12. https://doi.org/10.1016/j.exer.2016.07.011

Wang, S. K., & Chang, R. T. (2014). An emerging treatment option for glaucoma: Rho kinase inhibitors. *Clinical Ophthalmology*, 8, 883–890. https://doi.org/10.2147/OPTH.S41000

Zhang, L., Yu, D., Hu, M., Xiong, S., Lang, A., Ellis, L. M., & Pollock, R. E. (2000). Wild-type p53 suppresses angiogenesis in human leiomyosarcoma and synovial sarcoma by transcriptional suppression of vascular endothelial growth factor expression. *Cancer Research*, 60(13), 3655–3661.

Zhao, X., Ramsey, K. E., Stephan, D. A., & Russell, P. (2004). Gene and protein expression changes in human trabecular meshwork cells treated with transforming growth factor-beta. *Investigative Ophthalmology and Visual Science*, 45(11), 4023–4034. https://doi.org/10.1167/iovs.04-0535

SUPPORTING INFORMATION

Additional Supporting Information may be found online in the supporting information tab for this article.